J. Plasma Fusion Res. SERIES, Vol. 2 (1999) 339–342

Automatic Chase of Low-Pressure Vortex Axes

ADACHI Takahiro*, MIURA Hideaki[1] and KIDA Shigeo[1]
Doshisha Univ., Kyotanabe, Kyoto 610-0321, Japan
[1]*National Institute for Fusion Science Toki, Gifu 509-5292, Japan*

(Received: 18 December 1998 / Accepted: 25 February 1999)

Abstract

A new method by which the motion of the axis of a low-pressure vortex is chased automatically is developed for the purpose of understanding of vortical dynamics. An equation which describes the temporal evolution of a vortex axis is derived and solved numerically. This method is applied to a flow field composed of two interacting pairs of anti-parallel vortex tubes to visualize their reconnection process.

Keywords:

automatic chase, low-pressure vortex, vortex axis, reconnection

1. Introduction

It is commonly recognized that coherent structures such as vortex tubes and layers exist in fully developed turbulence and believed that they may play essential roles in turbulence dynamics. In order to investigate their dynamics, it is necessary to develop an efficient method to educe their structure and to trace their temporal evolution in complicated flows. In this paper, we present an automatic method for chasing a low-pressure vortex [1,2]. This method is successfully applied to a flow field composed of two pairs of anti-parallel vortices placed orthogonally to each other.

2. Formulation

We derive here an equation which describes the temporal evolution of the axis of a low-pressure vortex. Let us define the eigenvalues $\lambda^{(i)}$ $(i = 1, 2, 3)$ of pressure Hessian $H_{ab} = \partial^2 p/\partial x_a \partial x_b$ $(a, b = 1, 2, 3)$ and the associated eigenvectors $e_a^{(i)}$ by

$$H_{ab}\, e_b^{(i)} = \lambda^{(i)} e_a^{(i)}, \quad e_a^{(i)} e_a^{(i)} = 1, \tag{1}$$

where the summation convention is assumed for repeated subscripts. Since H_{ab} is a symmetric tensor, all of the three eigenvalues are real. Then, we assume, without loss of generality, that $\lambda^{(1)} \geq \lambda^{(2)} \geq \lambda^{(3)}$. The axis of a low-pressure vortex is defined as such a line on which the pressure p takes a local minimum in cross-sections normal to the third eigenvector $e_a^{(3)}$ of H_{ab}. If the pressure-gradient is normalized as $|\nabla \hat{p}| = 1$, then we have the identity,

$$e_a^{(3)} = \frac{\partial \hat{p}}{\partial x_a}, \tag{2}$$

on the vortex axis, where $\hat{p}$ denotes the normalized pressure. The direction of $e_a^{(3)}$ is chosen so that it makes an acute angle with $\partial \hat{p}/\partial x_a$.

The time derivative D/Dt taken as moving with a vortex axis is expressed as

$$\frac{D}{Dt} \equiv \frac{\partial}{\partial t} + \frac{\mathrm{d}x_a}{\mathrm{d}t}\frac{\partial}{\partial x_a}, \tag{3}$$

where $x_a = x_a(t)$ represents the position of the axis and $\mathrm{d}x_a/\mathrm{d}t$ its translational velocity. Differentiating eq. (2) with respect to time and using eq. (3), we obtain the equation for the translational velocity as

Corresponding author's e-mail: adach@me.saga-u.ac.jp
**Present address: OTEC Lab. Saga Univ., Saga 840-8502, Japan.*

$$\frac{\mathrm{d}x_b}{\mathrm{d}t}\left(\frac{\partial e_a^{(3)}}{\partial x_b}-H_{ab}\right)=\frac{\partial^2\hat{p}}{\partial t\partial x_a}-\frac{\partial e_a^{(3)}}{\partial t}. \qquad (4)$$

As will be shown in Appendix, the second-order tensor $\partial e_b^{(3)}/\partial x_a$ is written as

$$\frac{\partial e_b^{(3)}}{\partial x_a}=\sum_{j=1}^{2}\left(\frac{1}{\lambda^{(3)}-\lambda^{(j)}}\frac{\partial H_{mn}}{\partial x_a}e_m^{(j)}e_n^{(3)}\right)e_b^{(j)}. \qquad (5)$$

The temporal evolution of a vortex axis is obtained by solving eq. (4), in which the translational velocity is expressed only in terms of information of the pressure field.

3. Numerical Method

Here, we take two snapshots at t and $t+\Delta t$, say, from a time series of the pressure field, which is obtained by direct numerical simulation of the Navier-Stokes equation. Then we describe how to predict a new position at $t+\Delta t$ of a vortex axis which was picked up arbitrarily at t by the use of eq. (4).

3.1 Finite-difference approximation of time derivative

The time derivative in eq. (4) is approximated by the first-order finite difference in terms of field quantities at successive times t and $t+\Delta t$ as

$$\frac{\partial^2\hat{p}}{\partial t\partial x_a}=\frac{\partial\hat{p}^{t+\Delta t}/\partial x_a-\partial\hat{p}^{t}/\partial x_a}{\Delta t}, \qquad (6)$$

$$\frac{\partial e_a^{(3)}}{\partial t}=\frac{e_a^{(3)t+\Delta t}-e_a^{(3)t}}{\Delta t}, \qquad (7)$$

where $\hat{p}^t$ and $e_a^{(3)t}$ denote the normalized pressure and the third eigenvector at t. The difference of eqs. (6) and (7) yields the right-hand side of eq. (4) as

$$\frac{\partial^2\hat{p}}{\partial t\partial x_a}-\frac{\partial e_a^{(3)}}{\partial t}=\frac{\partial\hat{p}^{t+\Delta t}/\partial x_a-e_a^{(3)t+\Delta t}}{\Delta t}, \qquad (8)$$

where use has been made of the relation,

$$e_a^{(3)t}=\frac{\partial\hat{p}^t}{\partial x_a}, \qquad (9)$$

which follows from eq. (2).

3.2 Automatic chase

An automatic chase of vortex axes from t to $t+\Delta t$ is carried out according to the following steps:

[1] At time t, choose a vortex axis $\boldsymbol{C}^t$ which is constructed by connecting nearest-neighboring candidate points until there are no more candidates within two grid sizes in each of the three coordinate axes. Here, candidate points are such points on which $\lambda^{(2)}>0$ and a swirl condition are satisfied [1,2] (see Fig. 1).

[2] Predict the position at $t+\Delta t$ of each candidate point of the vortex axis chosen in step [1] by the use of eq. (4) for the translational velocity. A set of these new positions is denoted by $\boldsymbol{P}^{t+\Delta t}$.

[3] Find first a grid point which is closest to each element in $\boldsymbol{P}^{t+\Delta t}$, then a candidate point which is located within one grid-size from it in each of the three coordinate axes, and which satisfies those conditions given in step [1]. A set of these new candidate points is denoted by $\boldsymbol{C}'^{t+\Delta t}$.

[4] Connect each element in $\boldsymbol{C}'^{t+\Delta t}$ with its nearest-neighbors if they are located within two grid-sizes in each of the three coordinate axes, and finish it otherwise. In this process, a point which does not belong to $\boldsymbol{C}'^{t+\Delta t}$ may sometime be connected. The union of $\boldsymbol{C}'^{t+\Delta t}$ and these extra candidate points is denoted by $\boldsymbol{C}''^{t+\Delta t}$. The length of resultant $\boldsymbol{C}''^{t+\Delta t}$ is in general different from that of $\boldsymbol{C}^t$ because separation and reconnection of vortex axes may occur.

[5] Pick up only such sequences of points of $\boldsymbol{C}''^{t+\Delta t}$ that include at least two elements belonging to $\boldsymbol{C}'^{t+\Delta t}$. This condition should be introduced so as to exclude a false termination caused by unavoidable numerical errors. This condition is satisfied for the left one of the two parts of $\boldsymbol{C}''^{t+\Delta t}$ shown in Fig. 1 but not for the right. Therefore, the latter is discarded, while the former is retained and identified as a vortex axis $\boldsymbol{C}^{t+\Delta t}$ which has evolved from $\boldsymbol{C}^t$.

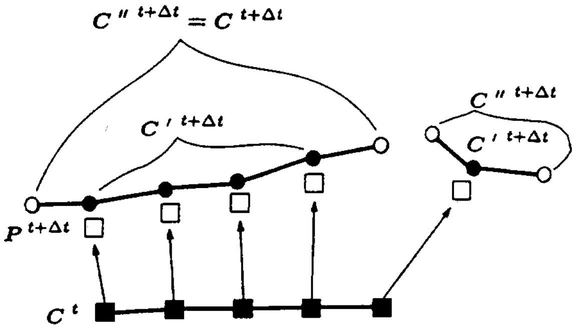

Fig. 1 Sets of points in each step in the method of automatic chase of vortex axes. ■, $\boldsymbol{C}^t$, a vortex axis at t; □, $\boldsymbol{P}^{t+\Delta t}$, predicted points at $t+\Delta t$; ●, $\boldsymbol{C}'^{t+\Delta t}$, candidate points; ○-●-●-----●-○, $\boldsymbol{C}''^{t+\Delta t}$, union of $\boldsymbol{C}'^{t+\Delta t}$ and extra points; $\boldsymbol{C}^{t+\Delta t}$, vortex axis at $t+\Delta t$ which has evolved from $\boldsymbol{C}^t$.

4. Application to a Pair of Anti-Parallel Vortices

In order to examine the vortex interaction as well as to check our new method described in the preceding section, the method of automatic chase of vortex axes is applied to a flow field which is obtained by the direct numerical simulation of the Navier-Stokes equation. The Fourier spectral method with resolution of 64^3 is used in a periodic cube of period 2π.

As the initial condition we take two pairs of anti-parallel vortex tubes which are placed orthogonally to each other. The vorticity distribution across each tube is given by the Gaussian distribution as

$$\begin{aligned}\omega_x &= \omega_0 \exp[-a\{(y-y_0)^2+(z+z_0)^2\}] \\ &\quad - \omega_0 \exp[-a\{(y+y_0)^2+(z+z_0)^2\}], \\ \omega_y &= -\omega_0 \exp[-a\{(x-x_0)^2+(z-z_0)^2\}] \\ &\quad + \omega_0 \exp[-a\{(x+x_0)^2+(z-z_0)^2\}], \\ \omega_z &= 0 \end{aligned} \tag{10}$$

where, $a = 50$, $\omega_0 = 100/\pi$, $x_0 = y_0 = 3\Delta x$, and $\Delta x = 2\pi/64$ is the grid size. The circulation around each tube is $\Gamma = \omega_0\pi/a = 2$. The vortex Reynolds number is then given by $Re_\Gamma = \Gamma/\nu = \omega_0\pi/a\nu = 200$, where $\nu = 0.01$ is the kinematic viscosity of fluid. The motion of low-pressure vortex axes is traced by the present method of automatic chase every $\Delta t = 0.1$ time unit.

The temporal evolution of the vortex axes at $t = 0,1,5$ is represented in Figs. 2(a)-(c). In each figure, we display the loci of the sectionally local minimum of pressure together with the edge of the periodic cube. Two pairs of vortices are placed orthogonally to each other at the initial instant (Fig. 2(a)). Each pair of vortices travel perpendicularly to the other by their own induced velocity and the two pairs approach each other. At their closest positions, each pair is bended by the repulsive velocity induced by the other as shown in Fig. 2(b). In the meanwhile, parts of two vortices which belong to different pairs approach each other with aligning their vorticity anti-parallel. Cancellation of anti-parallel vorticity by viscous diffusion then becomes effective, which causes vortex reconnections to change topology of the vortex axes (Fig. 2(c)). As a result, the two pairs of anti-parallel vortices pass through each other and are cut into four separate vortices (cf. Figs. 2(a) and (c)).

5. Conclusions

We have derived equations which describe the

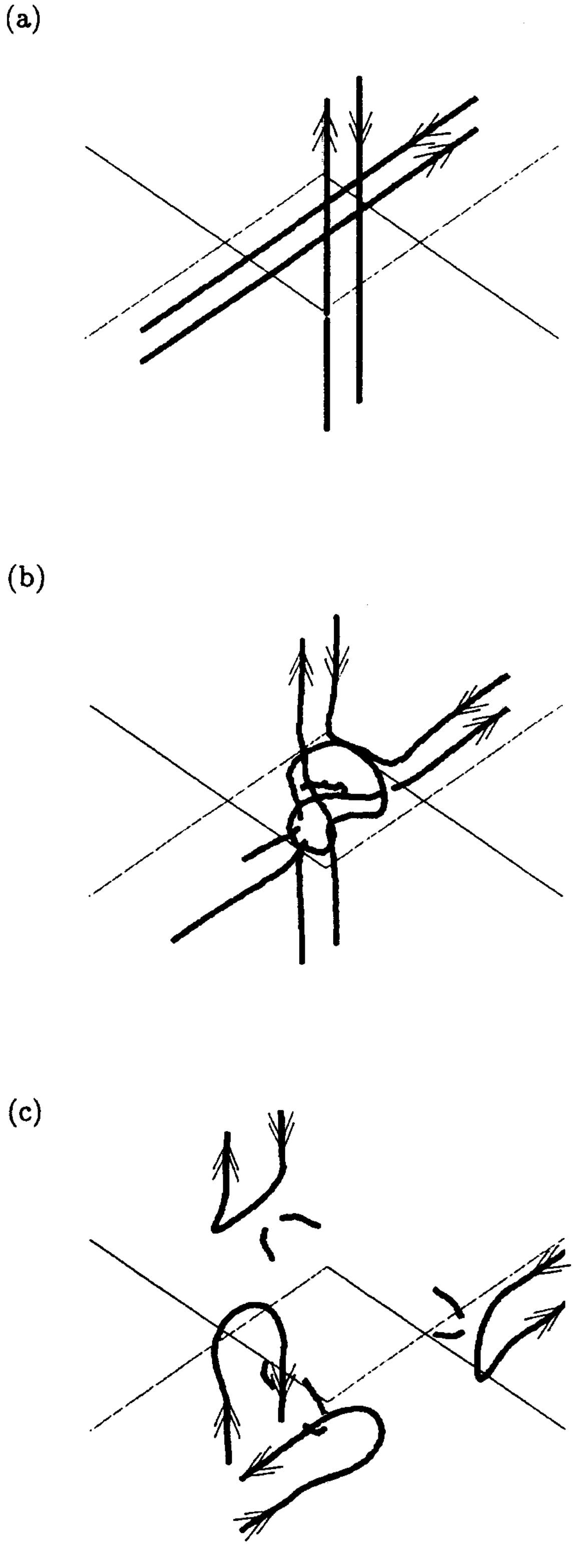

Fig. 2 Interaction of two pairs of anti-parallel vortex tubes placed orthogonally to each other. (a) $t = 0$, (b) $t = 1$, (c) $t = 5$. Double arrows denote the direction of vorticity.

temporal evolution of the axis of a low-pressure vortex and developed a new method which chases its axis automatically. It was successfully applied to a system of two pairs of anti-parallel vortex tubes to visualize a sequence of the vortex reconnections clearly.

References

[1] H. Miura and S. Kida, J. Phys. Soc. Jpn. **66**, 1331 (1997).

[2] S. Kida and H. Miura, J. Phys. Soc. Jpn. **67**, 2166 (1998).

Appendix

We derive here expression (5) of $\partial e_b^{(3)}/\partial x_a$. It follows from definition (1) that

$$\lambda^{(i)} = e_a^{(i)} H_{ab}\, e_b^{(i)}, \tag{11}$$

which, after differentiating with respect to x_c, leads to

$$\begin{aligned}\frac{\partial \lambda^{(i)}}{\partial x_c} &= \frac{\partial e_a^{(i)}}{\partial x_c} H_{ab}\, e_b^{(i)} + e_a^{(i)} \frac{\partial H_{ab}}{\partial x_c} e_b^{(i)} + e_a^{(i)} H_{ab} \frac{\partial e_b^{(i)}}{\partial x_c} \\ &= \lambda^{(i)} \frac{\partial e_a^{(i)}}{\partial x_c} e_a^{(i)} + e_a^{(i)} \frac{\partial H_{ab}}{\partial x_c} e_b^{(i)} + \lambda^{(i)} e_b^{(i)} \frac{\partial e_b^{(i)}}{\partial x_c} \\ &= e_a^{(i)} \frac{\partial H_{ab}}{\partial x_c} e_b^{(i)},\end{aligned} \tag{12}$$

where use has been made of eq. (1) and the orthogonality between $\partial e_a^{(i)}/\partial x_c$ and $e_a^{(i)}$. A differentiation of the first of eq. (1) with respect to x_c, on the other hand, leads to

$$\frac{\partial H_{ab}}{\partial x_c} e_b^{(i)} + H_{ab} \frac{\partial e_b^{(i)}}{\partial x_c} = \frac{\partial \lambda^{(i)}}{\partial x_c} e_a^{(i)} + \lambda^{(i)} \frac{\partial e_a^{(i)}}{\partial x_c}. \tag{13}$$

On substitution of eq. (12) into eq. (13), we obtain

$$\begin{aligned}(H_{ab} - \lambda^{(i)}\delta_{ab}) \frac{\partial e_b^{(i)}}{\partial x_c} &= e_m^{(i)} \frac{\partial H_{mn}}{\partial x_c} e_n^{(i)} e_a^{(i)} \\ &\quad - \frac{\partial H_{ab}}{\partial x_c} e_b^{(i)}.\end{aligned} \tag{14}$$

An inner product of eq. (14) and $e_a^{(j)}$ ($j = 1, 2, 3, j \neq i$) gives

$$(\lambda^{(j)} - \lambda^{(i)}) e_b^{(j)} \frac{\partial e_b^{(i)}}{\partial x_c} = - e_a^{(j)} \frac{\partial H_{ab}}{\partial x_c} e_b^{(i)}, \ (i \neq j), \tag{15}$$

where $e_a^{(i)} e_a^{(j)} = \delta_{ij}$ has been used. Since $\partial e_b^{(i)}/\partial x_c$ is orthogonal to $e_b^{(i)}$, then $\partial e_b^{(i)}/\partial x_c$ should be written in terms of the other two components (eq. (15)) of $e_b^{(j)}$ ($j \neq i$). Thus, we finally find that

$$\frac{\partial e_b^{(i)}}{\partial x_a} = \sum_{\substack{j=1 \\ (j \neq i)}}^{3} \left(\frac{1}{\lambda^{(i)} - \lambda^{(j)}} \frac{\partial H_{mn}}{\partial x_a} e_m^{(j)} e_n^{(i)} \right) e_b^{(j)}, \tag{16}$$

as long as $\lambda^{(i)} \neq \lambda^{(j)}$ for $i \neq j$.